energies

Article

Research on Interruption Performance of Environmentally Friendly C_4F_7N Mixed-Gas-Insulated Switchgear

Chenxi Bian [1], Baina He [1,*], Xin Lin [2], Yujia Liu [1], Hui Lou [1], Lingzhe Kong [1], Xueting Dai [1], Shuo Wu [1], Fantao Meng [1] and Yang Liu [1]

1 College of Electric and Electronic Engineering, Shandong University of Technology, Zibo 255000, China
2 Key Laboratory of Special Machine and High Voltage Apparatus, Ministry of Education, Shenyang University of Technology, Shenyang 110000, China
* Correspondence: hebaina@sdut.edu.cn

Abstract: SF_6, which is currently widely used in gas-insulated power transmission equipment, is a greenhouse gas with a very strong greenhouse effect. Therefore, developing environmentally friendly gas insulation equipment to gradually reduce the use of SF_6 has become a hot research topic. As the most potential alternative gas, C_4F_7N is of great significance to study the electrical characteristics of the medium-voltage switching field to promote the green development of the power industry. Based on multi-physical field coupling to construct the 40.5 kV circuit breaker mode, this paper uses C_4F_7N/CO_2 mixed gas to compare and study the dynamic characteristics of a C_4F_7N/CO_2 mixed gas circuit breaker when breaking the short-circuit current and the dielectric recovery strength with no-load breaking, as well as to evaluate the electrical performance of C_4F_7N mixed gas in a 40.5 kV breaker with the gas breakdown criterion. The results show that mixing O_2 in a high current can improve the breaking performance of an environmental protection circuit breaker and increasing the C_4F_7N mass fraction can enhance the dielectric recovery strength of the environmentally friendly circuit breaker. Considering the overall performance of the gas, the 5%C_4F_7N/90% CO_2/5%O_2 mixed gas has some alternative potential.

Keywords: eco-friendly insulating gas; self-blasting circuit breaker; multi-physics coupling; dielectric recovery property; C_4F_7N

check for updates

Citation: Bian, C.; He, B.; Lin, X.; Liu, Y.; Lou, H.; Kong, L.; Dai, X.; Wu, S.; Meng, F.; Liu, Y. Research on Interruption Performance of Environmentally Friendly C_4F_7N Mixed-Gas-Insulated Switchgear. *Energies* **2022**, *15*, 6500. https://doi.org/10.3390/en15186500

Academic Editor: Antonis A. Zorpas

Received: 12 August 2022
Accepted: 1 September 2022
Published: 6 September 2022

1. Introduction

As an insulating gas, SF_6 is widely used in high voltage switchgear. However, SF_6 has a serious greenhouse effect, and its global warming potential is about 23,900 times that of CO_2 [1,2]. Therefore, finding an environmentally friendly insulating gas is one of the important problems to be solved in the field of high-voltage switches [3,4]. At present, the research hotspot of a SF_6 substitute gas has developed from the original SF_6 mixed gas to the new substitute gases $C_5F_{10}O$ and C_4F_7N. Among them, C_4F_7N is a new type of insulating gas developed by 3M. The insulating performance of pure C_4F_7N is twice that of SF_6, and the ozone depletion potential value is 0 [5–8]. Due to its high boiling point, C_4F_7N is very easy to be liquefied under low-temperature conditions, so it must be mixed with conventional gas to reduce the liquefaction temperature before it can be used in power equipment with high inflation pressure and in extremely cold regions [9–11].

At present, the conventional buffer gases include CO_2 and N_2. Some researchers have studied the insulating properties of the mixed gases C_4F_7N/CO_2 and C_4F_7N/N_2 [12,13], which has laid down the basis for the application of the C_4F_7N mixed gas. To investigate the effects of different buffer gases on the C_4F_7N mixed gases, experiments are carried out to study the DC breakdown characteristics of the C_4F_7N mixed gases in some works. Their research results show that the synergistic effect of the C_4F_7N/CO_2 mixed gas is better than that of the C_4F_7N/N_2 mixed gas, which also indicates that the C_4F_7N/CO_2 mixed gas with a mass fraction of 7% to 13% has the potential to replace SF_6 [14–17]. As for sensitivity to the non-uniformity of the electric field of the C_4F_7N mixed gas, some scholars conducted experimental research on the breakdown characteristics of different electrodes. The results show that the C_4F_7N mixed gas had higher sensitivity to the non-uniformity of the electric field than SF_6, and they needed to increase the mass fraction of C_4F_7N to improve its insulation strength, so as to reduce its sensitivity to the non-uniformity of the electric field [18–20]. Therefore, some progress has been achieved in research on the insulation and decomposition characteristics of C_4F_7N mixed gas. However, there are few studies on the arc extinguishing and breaking characteristics of C_4F_7N mixed gas, and the dynamic characteristics of the arc are mainly investigated via experiments [21,22]. The breaking experiment of a circuit breaker is not only time-consuming and expensive, but it is also difficult to obtain some internal parameters of the arc plasma. However, with the development of CFD (computational fluid dynamics) and MHD, numerical simulation has become an alternative to the breaking experiment. Many scholars have calculated the physical property parameters of arc plasma of the C_4F_7N mixed gas, which has laid down the basis for the MHD simulation [23]. According to the current research situation of C_4F_7N, the C_4F_7N/CO_2 mixed gas has great potential as a substitute gas of SF_6 which is expected to be applied in the medium- and low-voltage fields. However, compared with studies on the insulation characteristics of the C_4F_7N mixed gas, research on the arc extinguishing characteristics of C_4F_7N mixed gas is still limited [24]. Therefore, it is necessary to study the development patterns of an arc in the arc extinguishing chamber under the nozzle of the actual circuit breaker and the influencing factors on the breaking performance. The 40.5 kV self-blasting circuit breaker is widely used in 35 kV distribution lines, which has great promotion and application potential and can provide a basis for the development of high breaking capacity circuit breakers. The self-blasting circuit breaker utilizes the energy of the arc burning to increase the air pressure in the expansion chamber, so as to form a pressure difference to achieve arc extinguishing, which can reflect the influence of gas properties on the breaking performance. Therefore, our work selects the 40.5 kV self-blasting circuit breaker as the research object to study the interruption performance of the environmentally friendly insulating gas under the existing circuit breaker structure. The factors affecting the interruption performance of circuit breakers are analyzed to provide a basis for the production of environmentally friendly gas-insulated circuit breakers.

In this paper, a two-dimensional MDH arc model is constructed based on multi-physics coupling, which is used to simulate and calculate the arc temperature and pressure distribution when the environmentally friendly circuit breaker is breaking a short-circuit current, and the dynamic characteristics of the arc are also analyzed. The air flow field and electric field distributions of the arc extinguishing chamber during the no-load breaking process of the environmentally friendly circuit breaker were calculated. Then, by combining the air flow field and electric field calculation results, the dielectric recovery strengths of the C_4F_7N/CO_2 mixed gases with different proportions under the 40.5 kV circuit breaker structure was analyzed. Finally, the breaking performance of the C_4F_7N/CO_2 mixed gas was evaluated according to the dynamic characteristics of the arc under breaking a short-circuit current and the no-load dielectric recovery strength.

2. Circuit Breaker Interruption Model

2.1. Arc MHD Model

The dynamic process in the circuit breaker arc combustion process can be described by N-S equations, electromagnetic field equations, turbulence models, and radiation models. The arc MHD equation is established on the basis of the N-S equation by adding specific source terms, which are described as follows:

Mass Conservation Equation:

$$\frac{\partial \rho}{\partial t} + \nabla \cdot (\rho u) = 0 \tag{1}$$

Axial momentum conservation equation:

$$\frac{\partial(\rho u_z)}{\partial t} + \nabla\cdot(\rho u u_z) = \nabla\cdot(\mu\nabla u_z) - \frac{\partial p}{\partial z} + S_z \tag{2}$$

$$S_z = J_r \times B \tag{3}$$

Radial momentum conservation equation:

$$\frac{\partial(\rho u_r)}{\partial t} + \nabla\cdot(\rho u u_r) = \nabla\cdot(\mu\nabla u_r) - \frac{\partial p}{\partial r} + S_r \tag{4}$$

$$S_r = J_z \times B \tag{5}$$

Energy conservation equation:

$$\frac{\partial(\rho h)}{\partial t} + \nabla\cdot(\rho u h) = \nabla\cdot\left(\frac{k'}{C_p}\nabla h\right) + \sigma E^2 - q \tag{6}$$

Electromagnetic equations:

$$\nabla \times E = -\frac{\partial B}{\partial t} \tag{7}$$

$$\nabla \times B = \mu_0 J \tag{8}$$

$$J = \sigma(E + u \times B) \tag{9}$$

where ρ is density; u the velocity vector; J_r the radial current density; J_z the axial current density; u_r the radial velocity component; u_z the axial velocity component; μ the viscosity; k' the thermal conductivity; K the temperature; C_p the heat capacity; σ the electrical conductivity; E the electric field strength; B the magnetic induction; q the radiation source term; h the enthalpy; and μ_0 the magnetic permeability.

In the circuit breaker arc simulation, the above governing equations are solved by FLUENT, and the electromagnetic field equations are defined using user-defined scalars. The MHD equation is constructed and solved by adding a source term to the FLUENT standard equation. The governing equation parameters and source terms are shown in Table 1.

Table 1. The governing equation parameters and source terms.

Governing Equation	Φ	Γ_Φ	S_Φ
Mass	1	0	0
Axial momentum	u_r	μ	J_zB
Radial momentum	u_z	μ	J_rB
Energy	h	k/C_p	0
Electrical	φ	σ	σE^2-q
Electrical	A	μ_0	0

2.2. Turbulence Model

In the simulation process of circuit breaker breaking, the turbulent effect of the arc cannot be ignored. Turbulent flow conforms to the continuity assumption in fluid mechanics, so it can be directly solved numerically. However, the direct solution needs to be divided into very fine meshes, which requires a large amount of calculation. In order to simplify the calculation, the RANS (Reynolds-averaged Navier–Stokes, RANS) equation is usually used to solve the turbulent flow in an engineering simulation. In the arc simulation, the K-E equation in the RANS equation is highly practical. The K-E equation uses the K equation and the E equation to describe the turbulent dynamic viscosity. The specific description is as follows:

$$\rho\frac{\partial k}{\partial t} + \rho(u \cdot \nabla)k = \nabla \cdot \left[\left(\mu + \frac{\mu_t}{\sigma_k}\right)\nabla k\right] + P_k - \rho\varepsilon \tag{10}$$

$$\rho\frac{\partial \varepsilon}{\partial t} + \rho(u \cdot \nabla)\varepsilon = \nabla \cdot \left[\left(\mu + \frac{\mu_t}{\sigma_\varepsilon}\right)\nabla \varepsilon\right] + C_{\varepsilon 1}\frac{\varepsilon}{k}P_k - C_{\varepsilon 2}\rho\frac{\varepsilon^2}{k} \tag{11}$$

$$\mu_t = \frac{C_\mu \rho k^2}{\varepsilon} \tag{12}$$

According to the Reynolds-averaged energy equation:

$$k_t = \frac{C_p \mu_t}{\mathrm{Pr}_t} \tag{13}$$

where k is turbulent kinetic energy; ε the turbulent dissipation rate; μ_t the turbulent viscosity; k_t the turbulent heat transfer coefficient; C_p heat capacity; and ρ density.

2.3. Radiation Model

In the process of breaking a high current, radiation is the main method of arc energy dissipation. At present, four radiation models are mainly considered in the circuit breaker breaking simulation: the NEC (net emission coefficient, NEC) radiation mod, the P1 model, the local feature method, and the discrete coordinate method. Frank Reichert's group compared the effects of four radiation models on temperature distribution and points out that the NEC radiation model is the most practical [25]. The NEC radiation model is constantly being revised and improved. The researchers of the University of Liverpool revised the NEC model combined with the circuit breaker model and proposed a semi-empirical NEC model suitable for circuit breaker arc simulation [26]. In this simulation, the modified NEC model is used to calculate the arc heat radiation.

2.4. Geometric Model and Boundary Conditions

The simulation of this paper is based on the 40.5 kV self-blasting circuit breaker widely used at a 35 kV voltage level. The self-exploding circuit breaker can make full use of the energy when the arc burns to form a pressure difference between the expansion chamber and the nozzle to blow out the arc. The geometric model of the circuit breaker arc extinguishing chamber is shown in Figure 1. In the simulation, the initial temperature of the arc extinguishing chamber is 300 K. The short-circuit current is set to 31.5 kA, which is the rated short-circuit breaking current of the 40.5 kV self-blasting circuit breaker. The boundary condition settings are shown in Table 2.

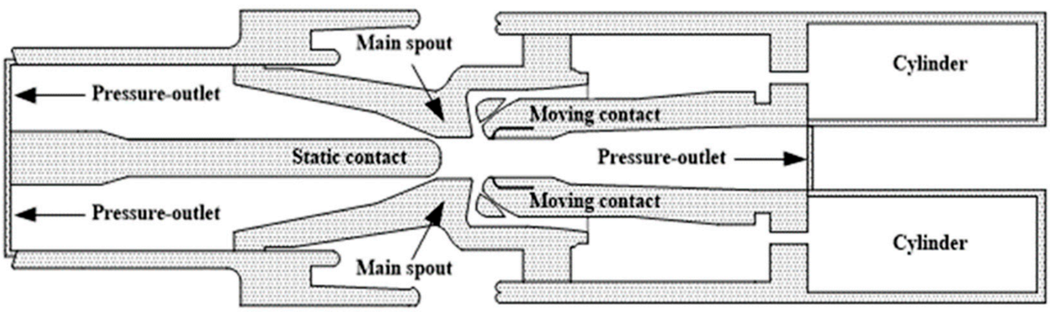

Figure 1. Geometric model of 40.5 kV circuit breaker.

Table 2. Boundary condition.

Boundary	V	T	UDS(0)	UDS(1)
Static contact	-	300 K	$J = J_{arc}$	A = 0
Moving contact	-	300 K	$\varphi = 0$	A = 0
Pressure outlet	0	300 K	$J = 0$	A = 0
Cylinder wall	0	300 K	$J = 0$	A = 0
Main spout	-	Coupled	$J = 0$	A = 0

For the gas flow field, the gas flow velocity is 0 m/s, and the interface between the fluid and the solid is set as the non-sliding wall boundary condition. In the simulation, the moving contact is set as the boundary condition of current density, and the static arc contact is grounded. The current density is determined by the following equation:

$$J_{arc} = \frac{I}{S_{arc}} \tag{14}$$

where J_{arc} is the current density applied by the contact; I the short-circuit current; and S_{arc} the arc cross-sectional area.

The moving contact is a moving part, and the moving speed refers to the actual contact stroke curve. The motion of parts is realized by dynamic mesh. In this paper, the laying dynamic mesh technology is used to deal with the mesh changes in the moving area. The simulation is based on local thermodynamic equilibrium and treats the arc as a magnetofluid. In order to improve the calculation efficiency, it is assumed that the arc in the arc extinguishing chamber is a two-dimensional axisymmetric structure.

3. Analysis of Arc Dynamic Characteristics of C_4F_7N Mixed Gas

Based on the arc burning simulation model of the circuit breaker, the temperature and pressure distribution in the arc extinguishing chamber of the environmentally friendly C_4F_7N mixed gas circuit breaker when breaking the rated short-circuit current is calculated.

3.1. Analysis of Dynamic Characteristics of Arc Temperature

The arc temperature distribution of the C_4F_7N mixed gas and SF_6 in the arc burning stage are shown in Figure 2. After the moving contact is separated from the static contact, a plasma arc is rapidly formed between the contacts. Affected by the Lorentz force and Joule heat, the arc core position accumulates a large number of charged particles and causes the electric arc to appear in an obvious high temperature region. In the initial stage of the arc burning, the arc is mainly developed at the end of the static contact, and the arc energy is diffused in the arc extinguishing chamber through thermal radiation and heat transfer.

During the breaking process of the circuit breaker, there is a certain stroke in the closed state. At this time, the moving arc contact and the static arc contact have not been separated, and a small part of the gas flows out through the contact gap due to the movement of the contact. Thus, there is no significant difference among the three gas arcs at 2 ms in Figure 2. After 2 ms, the moving contact begins to separate from the static contact, and the arc between the contacts begins to burn violently. At 4 ms, the current reaches the maximum value, and the arc burns violently between the moving contact and the static contact gap. At this time, the injected arc energy is the maximum, but the arc temperature is not the maximum value affected by energy accumulation and dissipation. It can be seen from Figure 2 that the arc core temperature of the SF_6 arc is the highest; the arc core area is larger; the temperature diffusion range is wider; and the heat transfer capacity is stronger. The large arc core area and strong heat transfer performance of the SF_6 arc are beneficial to increase the pressure in the expansion chamber and enhance the gas flow. The arc temperature reaches the maximum value at 6 ms; the maximum temperature of the SF_6 gas arc is about 19,600 K; and the maximum temperature of the C_4F_7N mixed gas arc with two different mixing ratios is about 15,000 K. According to the arc extinguishing principle of the self-blasting circuit breaker, it can be seen that a higher arc temperature is very beneficial to improve the breaking performance. When the current crosses zero at 9 ms, the arc energy is quickly taken away under the action of air blowing. According to the temperature distribution at 9 ms, the arc temperature of SF_6 drops below 1000 K between the moving contact and the static contact, the arc temperature of $5\%C_4F_7N/95\%CO_2$ mixed gas drops to about 10,000 K, and the arc temperature of $5\%C_4F_7N/90\%CO_2/5\%O_2$ drops to 8000 K.

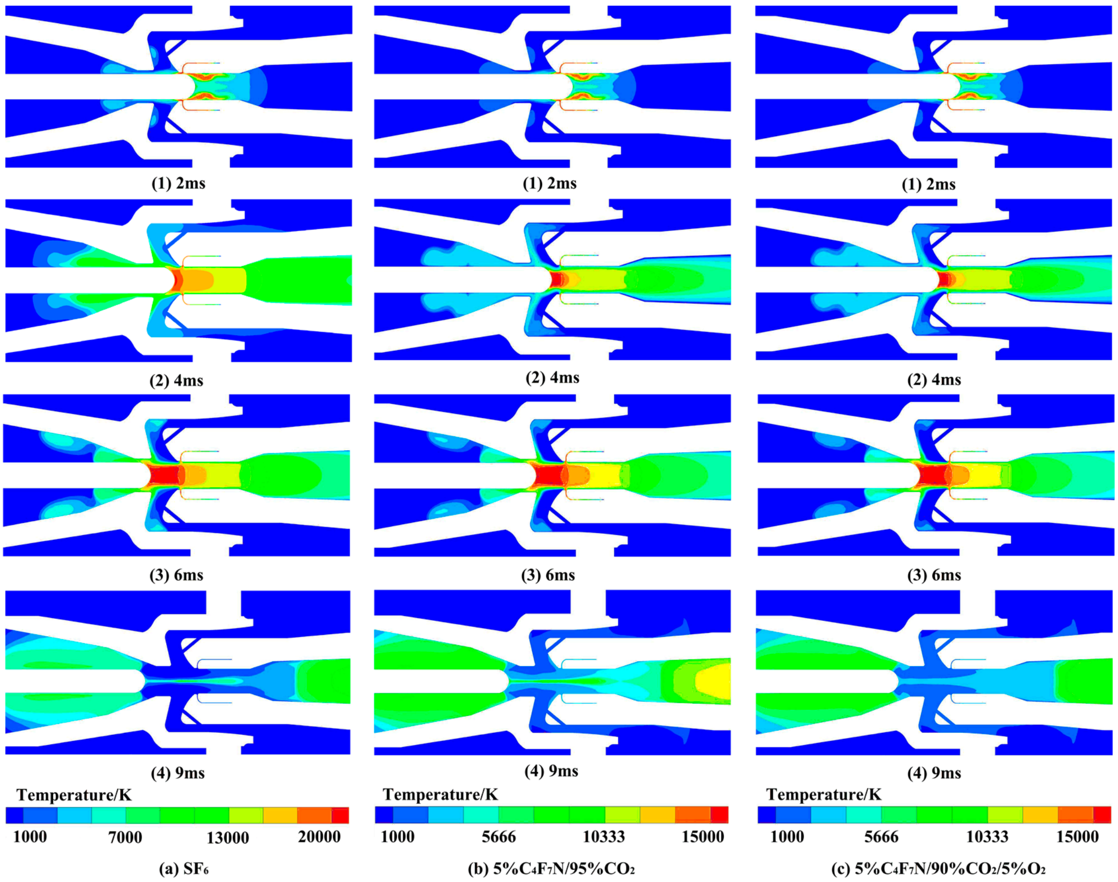

Figure 2. Arc temperature dynamic distribution.

On the basis of the assumption of local thermodynamic equilibrium, the arc electrical conductivity is positively correlated with the temperature. Therefore, the dielectric strength of the SF_6 arc after the arc is higher than that of the C_4F_7N mixed gas, and it is not easy to re-ignite after the arc. Among them, the post-arc dielectric strength of the $5\%C_4F_7N/90\%CO_2/5\%O_2$ mixed gas is higher than that of $5\%C_4F_7N/95\%CO_2$.

3.2. Dynamic Characteristics of Air Pressure in Arc Extinguishing Chamber

According to the breaking principle of a self-blasting circuit breaker, during the arc burning, the arc continuously heats up the gas in the expansion chamber, which increases the pressure in the expansion chamber. At the moment when the current is over zero, the main nozzle is opened. Because the pressure difference between the expansion chamber and the main nozzle forms a strong air blow, the accelerated arc energy dissipation makes the arc extinguished. Therefore, the analysis of the air pressure dynamic characteristics of the circuit breaker arc extinguishing chamber is conducive to the assessment of the eco-friendly insulating gas interruption performance.

Figure 3 shows the cloud diagram of the pressure distribution in the arc extinguishing chamber during the breaking process. After the moving contact and the static contact are separated, the arc is generated in the contact gap. Because the auxiliary nozzle and the main nozzle are blocked, the pressure propagates in the axial direction of the static contact, resulting in the pressure rise from the end of the static contact to the right pressure outlet area. At this time, the maximum pressure area is from the end of the static contact to the right pressure outlet, and the gas flows into the expansion chamber from the end of the static contact through the nozzle channel. With the increase in the contact gap, the auxiliary nozzle gradually opens, and the pressure in the expansion chamber continues to rise under the continuous heating of the arc. At the same time, the pressure at the end of the static contact decreases gradually, and the pressure difference between the expansion chamber and the end of the static contact decreases gradually. When the air pressure in the expansion chamber is greater than that at the end of the static contact, the air flow will begin to flow out from the expansion chamber to the nozzle, forming a blowing arc in the longitudinal direction and accelerating the dissipation of arc energy. The average air pressure in the expansion chamber is monitored in the simulation, as shown in Figure 4.

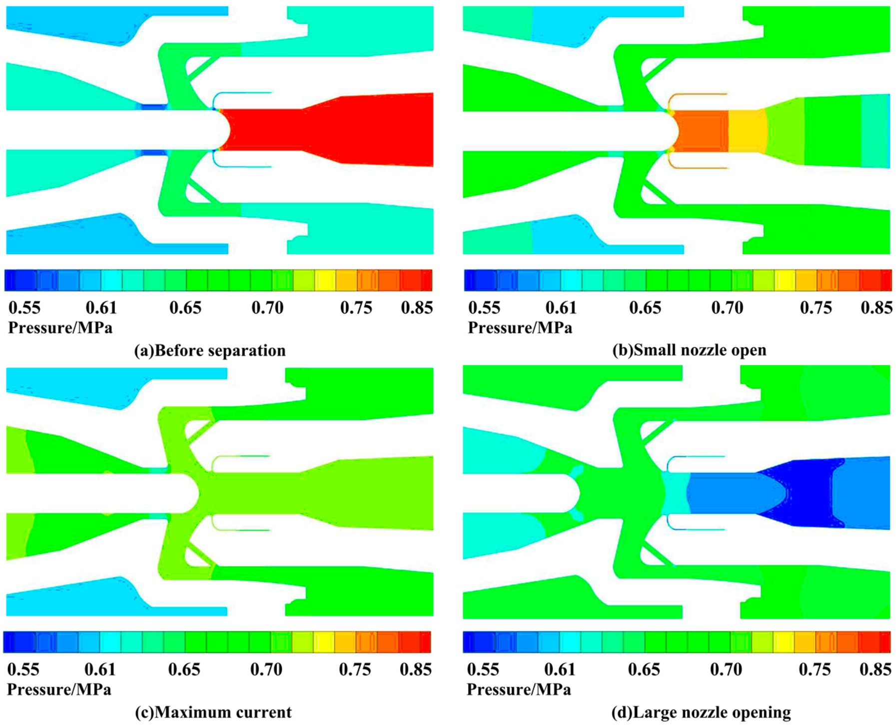

Figure 3. Dynamic pressure distribution of arc extinguishing chamber.

It can be seen from Figure 4 that when the insulating medium is SF_6 gas, the peak pressure in the expansion chamber is the largest, because SF_6 has excellent heat transfer performance in the arc burning stage, which can continuously heat the gas in the expansion chamber and increase the pressure in the expansion chamber. The higher air pressure in the expansion chamber forms a larger pressure difference at the nozzle, and the energy of the arc plasma can be quickly taken away after the current crosses zero under the drive of the pressure difference. The pressure peak of the CO_2 expansion chamber is the smallest, followed by 5%C_4F_7N/95%CO_2 mixed gas. Due to the large proportion of CO_2 in the mixed gas of 5%C_4F_7N/95%CO_2, the difference between the pressure peaks in the expansion chamber of the two gases is small. The low-pressure peak makes it impossible to form a large pressure difference between the expansion chamber and the nozzle, resulting in the environmentally friendly insulating gas being unable to form a strong gas blowing effect at the time of current zero crossing, which affects the arc heat dissipation. After adding O_2, the air pressure in the expansion chamber increases slightly, so the arc temperature of the

$5\%C_4F_7N/90\%CO_2/5\%O_2$ mixed gas is lower than that of the $5\%C_4F_7N/95\%CO_2$ mixed gas at zero crossing time.

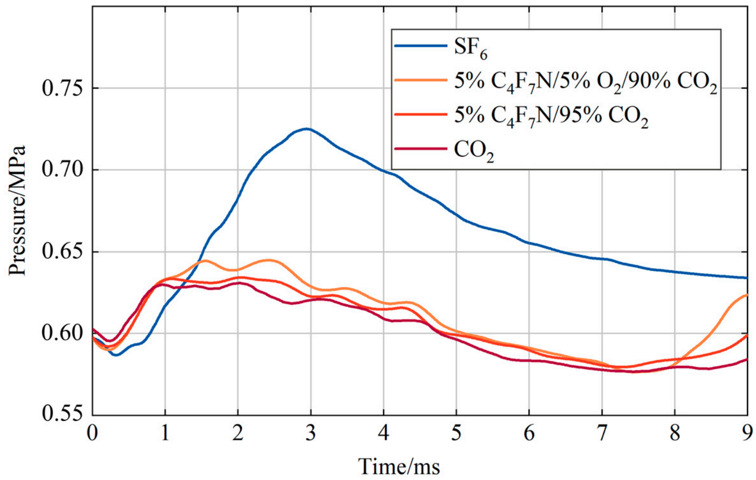

Figure 4. Pressure in the expansion chamber.

4. Dielectric Recovery Characteristics of Environmental Protection Circuit Breaker

When the circuit breaker interruption is a small current, the arc burning time between the contacts is short, and small contact spacing is prone to breakdown accidents under the action of TRV (transient recovery voltage). Therefore, it is necessary to study the dielectric recovery characteristic of circuit breakers when breaking small currents. Since the energy generated by the arc burning when breaking a small current can be taken away by the cold airflow in a very short time, this paper regards the dielectric recovery of a circuit breaker breaking a small current as the dielectric recovery process of no-load breaking.

4.1. Dielectric Recovery Calculation Model

In a quasi-uniform electric field, the gas breakdown process can be explained according to the streamer theory. According to the streamer theory, the strength of the entire electrical gap is calculated according to the weakest point of the electrical strength. Combined with the Pedersen breakdown criterion, the no-load breaking breakdown criterion of the circuit breaker is simplified to Equation (14):

$$K_1(E/N) \geq (E/N)^* \tag{15}$$

where K_1 is correction factor, (E/N) the ratio of electric field intensity to particle number per unit volume, and $(E/N)^*$ the critical breakdown field strength of gas.

According to the electromagnetic field theory, when $K_1(E/N) \leq (E/N)^*$ the voltage U_b that the air gap can withstand is proportional to the electric field strength between the air gaps. According to Avogadro's law, it can be known that the number of particles per unit volume N is inversely proportional to the relative molecular mass of the mixed gas and proportional to the density of the mixed gas, so the calculation formula for the recovery characteristics of the medium is derived.

$$U_b = \frac{K_1(E/N)^* R_0}{M} \frac{\rho}{E} \tag{16}$$

where U_b is the voltage withstood between air gaps, K_1 the correction factor, R_0 the Avogadro constant, M the relative molecular mass, ρ the density, and E the electric field intensity under unit voltage.

4.2. Electric Field Calculation Results

From Equation (16), it can be known that the maximum electric field intensity of the circuit breaker arc extinguishing chamber needs to be applied when a unit voltage is applied when calculating U_b. Therefore, this paper calculates the electric field distribution between the contacts during the breaking process of the circuit breaker. In the simulation, the static contact voltage is 1 V, and the moving contact is grounded. Since the relative dielectric constant of C_4F_7N mixed gas with different mass fractions has little difference, the same electric field distribution is given for C_4F_7N with different mass fractions.

Figure 5 shows the electric field distribution of the arc extinguishing chamber of circuit breakers at different disconnection distances. As can be seen from Figure 4, the electric field strength between the contacts is the largest due to the small spacing between the contacts and the static contacts at the time when they first separated. As the open distance between the contacts increases, the electric field strength between the contacts becomes smaller. In the initial stage of the separation between moving and static contacts, the maximum electric field intensity is mainly distributed in the static contact area. As the contact moves, the maximum electric field intensity begins to concentrate on the moving contact and the static contact end, and the maximum electric field strength area is distributed around the moving contact, static contact, and nozzle. From Equation (16), when the density is a fixed value, the greater the electric field strength is, the smaller the regional breakdown voltage is. Therefore, as the open distance increases, the medium recovery strength of the region between the moving arc contacts and the static arc contacts will be weaker compared with the other regions. Figure 5 shows the change curve of the maximum electric field strength of the arc chamber with different disconnection distances of the circuit breaker.

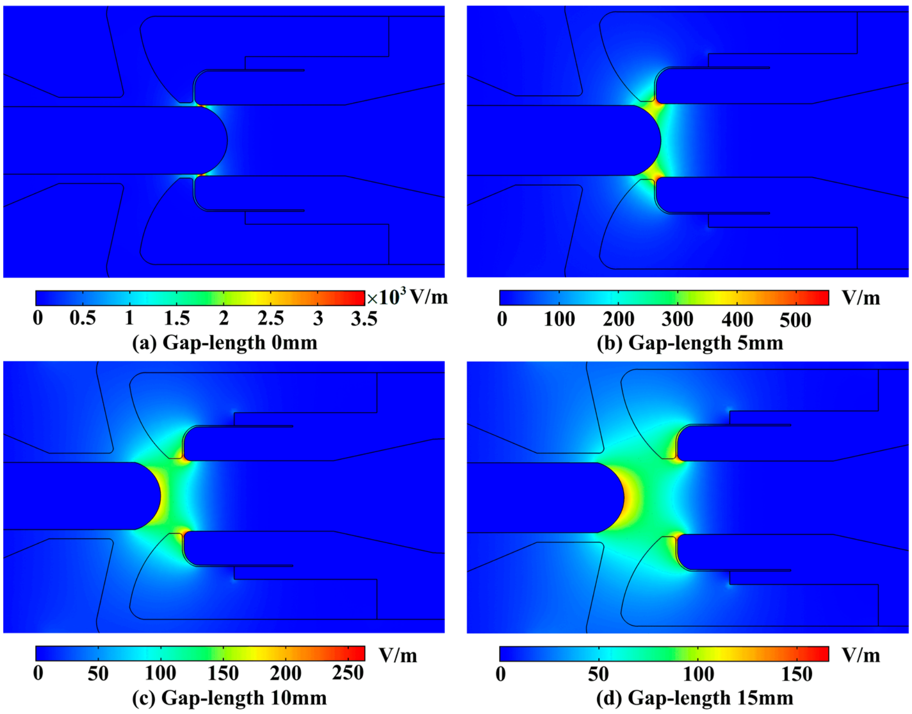

Figure 5. Electric field distribution of arc extinguishing chamber.

According to Figure 6, the electric field strength is maximum before the separation of the static contact and moving contact, and the maximum electric strength is 3504 V/m. When the disconnection distance is 10 mm, the maximum electric field strength decreases to 255 V/m, which is about 7% of the first moment of the separation. Before the disconnection distance is 10 mm, the maximum electric field strength has the largest change rate with the disconnection distance, and the average change rate is about 1051.45 $V{\cdot}m^{-1}ms^{-1}$; after a disconnection distance of 10 mm, the average rate of change in the maximum electric field intensity decreases. According to the calculation formula of the dielectric recovery characteristics, the large electric field strength between the contacts is not conducive to the dielectric recovery of the arc extinguishing chamber of the circuit breaker, and the rapid decrease in the maximum electric field strength can enhance the dielectric strength of the arc extinguishing chamber by increasing the value of ρ/E. When the circuit breaker breaks the small current, the arc burning time is short, the dynamic contact opening distance is small after the arc is extinguished, the electric field strength between the contacts is large, and the medium recovery strength is weak. Therefore, breakdown is prone in the action of transient recovery voltage.

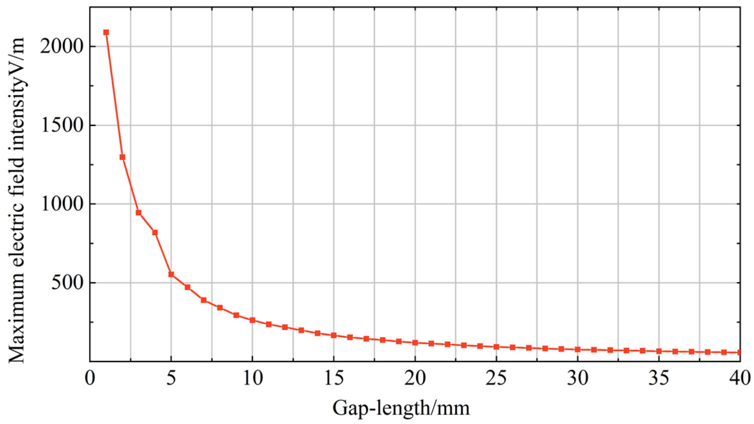

Figure 6. Electric field intensity change curve.

4.3. Calculation Results of No-Load Breaking Airflow Field

In this paper, the density distribution of circuit breakers under no-load conditions is calculated based on the N-S equation and the K-E turbulence equation, as shown in Figure 7.

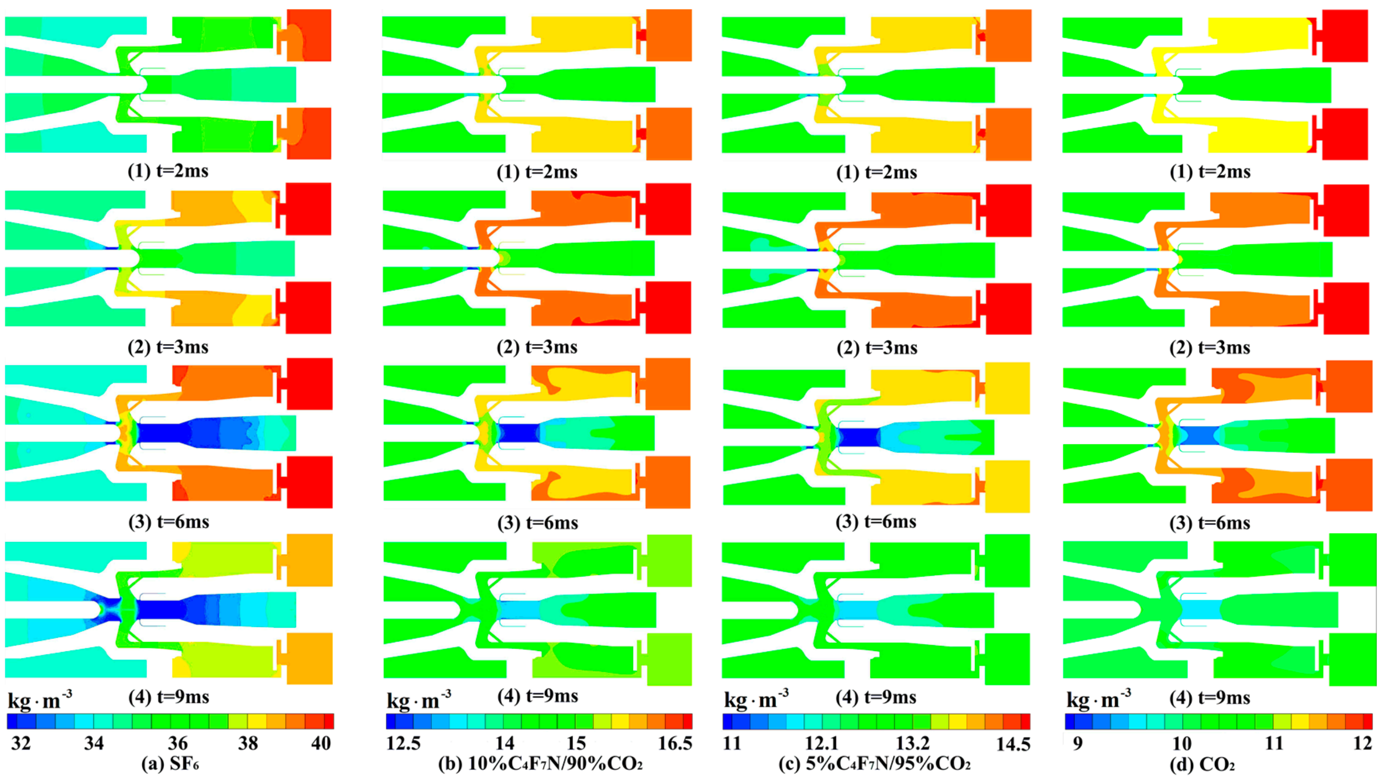

Figure 7. Arc extinguishing chamber density distribution cloud map.

From the gas state equation, the gas pressure is directly proportional to the gas density ρ. Therefore, the pressure distribution and the density distribution in the no-load breaking process of the circuit breaker are consistent, and the pressure and the density change can be analyzed uniformly. In Figure 7, before the moving contact is separated from the static contact, the gas density of the compressor chamber and the expansion chamber increases continuously with the cylinder compression as the large and small vents are blocked. At 2 ms, the contact can be separated, and due to the gap between the static contact and the nozzle, part of the gas can flow through the gap. After 2 ms, the contacts began to separate, the small nozzle gradually opened, and the gas begins to flow out of the pressure chamber through the small nozzle. At this time, the cylinder is still in the compression state, and the gas pressure and density of the compressor chamber still continue to increase. After the small nozzle is opened, the flow rate of the gas flow to this area increases due to the expansion area downstream of the small nozzle, resulting in the low-density area of the three-gas media downstream of the small nozzle position. According to the calculation formula of the dielectric recovery characteristics, the dielectric strength is the weakest in the low-density region. Therefore, when calculating the dielectric recovery strength, the moving contact and the static contact region ρ/E minimum value during the open contact process is mainly selected. After 6 ms, the large nozzle opens, the compressor chamber gas is released, and the gas density and pressure in the compressor chamber begin to decrease. As can be seen from Figure 7, the SF_6 can release for a long time after the large nozzle is opened, and the continuous airflow release can enhance the heat transfer capacity to extinguish the arc. With the flow injection theory, the electrical strength should be calculated according to the weakest point of the electrical strength. Therefore, the ρ/E minimum is used when calculating the gas medium. When E takes the maximum value and ρ takes the minimum value, ρ/E is the minimum. Figure 8 shows the SF_6, CO_2, and the C_4F_7N mixed gas minimum.

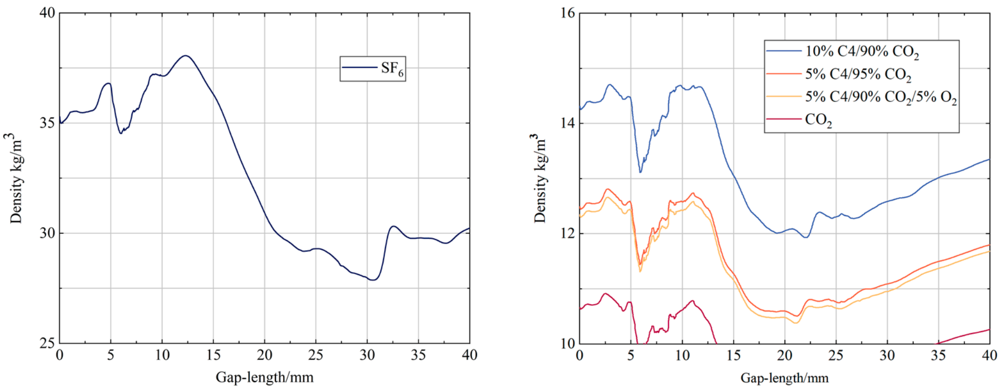

(**a**) SF_6 (**b**) C_4F_7N mixed gas

Figure 8. Curve of minimum density with gap length.

It can be seen from Figure 8 that the density of SF_6 is the highest and the density of CO_2 is the lowest among the five gaseous media. This is due to the large relative molecular mass of pure SF_6, resulting in a larger gas density under the same conditions. During the no-load breaking process of SF_6 gas, the minimum density of the arc extinguishing chamber has a minimum value of about 32 mm, and the C_4F_7N/CO_2 mixed gas has a minimum value of about 20 mm. Affected by the opening of the small nozzle at a distance of 5 mm, the density of the five gaseous media decreased. After the small nozzle is opened, the density of SF_6 is about 1.23 times the minimum value, and the C_4F_7N/CO_2 mixed gas is about 1.09 times the minimum value. This shows that C_4F_7N/CO_2 mixed gas is sensitive and susceptible to the disconnection mode.

4.4. Dielectric Recovery Characteristics

The dielectric recovery characteristics of 10%C_4F_7N/90%CO_2, 5%C_4F_7N/95%CO_2, and SF_6 are calculated in combination with the calculation results of electric field and gas flow field during no-load over breaking, as shown in Figure 9.

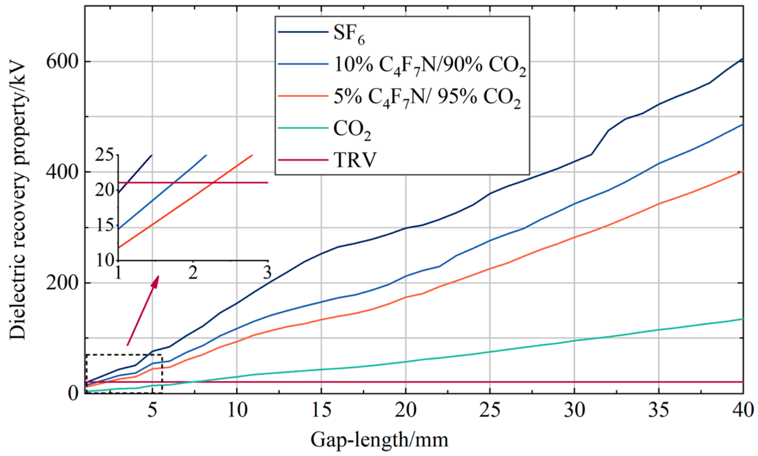

Figure 9. Dielectric recovery characteristics.

As shown in Figure 9, the dielectric recovery of SF_6 is higher than that of CO_2 and the C_4F_7N/CO_2 mixed gas under the same circuit breaker models, and the dielectric recovery strength of the C_4F_7N mixed gas increases with the increase in C_4F_7N mass fraction. When the opening distance is greater than 2.5 mm, the dielectric recovery characteristic U_b is greater than the (TRV) empirical value of 21.1 kV at a 35 kV voltage level. When the distance is greater than 5 mm, the U_b of the C_4F_7N mixed gas is about twice the TRV. This shows that if the arc can be extinguished after the distance of 5 mm, the probability of arc re-ignition is low, and a certain insulation margin can be maintained. The dielectric recovery characteristic U_b of CO_2 is greater than 21.1 kV when the gap length is 7.5 mm, and twice the empirical value of TRV when the gap length is 15 mm and the change rate of U_b when the gap length is small. It shows that when CO_2 gas is used as the arc extinguishing medium, the arc reburning rate is high after breaking the small current. In conclusion, under the same circuit breaker structure, the dielectric recovery strength of the C_4F_7N/CO_2 mixed gas is higher than that of CO_2. Therefore, compared with CO_2, the C_4F_7N/CO_2 mixed gas has more potential for substitution.

According to Equation (16), the dielectric recovery strength of gas media is related to the critical breakdown field strength of gas and the ρ/E minimum value. Since the same electric field distribution is used in this paper, the gaseous medium dielectric recovery strength is only related to the critical breakdown field strength and density distribution. The critical breakdown field strength in this paper refers to the calculation results in this research group and some other papers [27–29]. The critical breakdown field strength of the C_4F_7N mixed gas increases with the increase in the C_4F_7N mass fraction, and the insulating performance of the C_4F_7N mixed gas can be improved by adding O_2 [30]. Therefore, the incorporation of O_2 can enhance the dielectric recovery characteristics of environmentally friendly circuit breakers by increasing the critical breakdown field strength. During the no-load breaking process of the circuit breaker, the gas density distribution is mainly affected by the physical parameters. The physical parameters of the C_4F_7N mixed gas are related to the inflation pressure and the mixing ratio, so by changing the mixing ratio or the inflation pressure of the circuit breaker, the dielectric recovery characteristics of the environmentally friendly circuit breaker can be improved.

5. Conclusions

Based on the study of the arc dynamic characteristics and dielectric recovery characteristics of the environmentally friendly C_4F_7N mixed gas circuit breaker, the breaking performance of the environmentally friendly C_4F_7N mixed gas circuit breaker is evaluated. The specific research conclusions are as follows.

The existence of internal pressure difference in the expansion chamber of the circuit breaker can generate airflow to the arc core, and the cooling effect of the airflow accelerates the arc energy dissipation. When breaking the short-circuit current, the SF_6 arc core has the highest temperature and the strongest heat transfer ability, which causes a large pressure difference between the expansion chamber and the nozzle. The temperature of the SF_6 arc is lower than 4000 K at the time of current zero crossing, while the temperature of the C_4F_7N/CO_2 mixed gas arc is about 8000 K. After adding O_2 into the C_4F_7N/CO_2 mixture, the pressure difference between the expansion chamber and nozzle increases, the arc temperature decreases when the current crosses zero, and the dielectric strength increases after the arc is extinguished. The peak pressure of the CO_2 expansion chamber is the lowest, and the pressure difference between the expansion chamber and the nozzle is the smallest. The energy accumulation of CO_2 is caused by the failure of timely heat dissipation.

Under the same circuit breaker structure, the dielectric recovery strength of the three insulating gases is $SF_6 > C_4F_7N/CO_2 > CO_2$, where in the C_4F_7N/CO_2 mixed gas can maintain a sufficient insulation margin compared with CO_2 under the action of TRV. When the circuit breaker is no-load breaking, the C_4F_7N/CO_2 gas mixture can maintain sufficient insulation margin under the action of TRV. The dielectric recovery strength is affected by physical parameters and critical breakdown field strength, so that the dielectric recovery strength of the C_4F_7N/CO_2 gas mixture increases with the increase in C_4F_7N mass fraction. Considering the overall performance of the gas, the incorporation of O_2 can improve the dielectric recovery strength of the environmental protection circuit breaker by increasing the critical breakdown field strength of the C_4F_7N mixed gas. The arc extinguishing performance of the four gaseous media is $SF_6 > 5\%C_4F_7N/90\%CO_2/5\%O_2 > 5\%C_4F_7N/95\%CO_2 > CO_2$. During the interruption process, the mixed gas U_b of SF_6 and C_4F_7N/CO_2 can be more than twice the TRV empirical value after the gap length of 7.5 mm, and CO_2 can only reach the same level after the gap length of 17.5 mm. It can be seen that under the existing circuit breaker structure, the arc extinguishing performance of the C_4F_7N/CO_2 mixed gas is lower than that of SF_6, but better than that of pure CO_2 gas. After the arc is extinguished, the C_4F_7N/CO_2 mixed gas can maintain a sufficient insulation margin to prevent the arc re-igniting. The pressure difference between the expansion chamber and the nozzle can be increased by improving the structure of the arc extinguishing chamber and the arc extinguishing method to improve the arc extinguishing ability of the C_4F_7N binary mixed gas. Considering the properties of the gas comprehensively, the C_4F_7N/CO_2 mixed gas doped with O_2 has great application potential.

Author Contributions: Conceptualization, methodology, and writing, B.H. and C.B.; software, H.L.; validation, Y.L. (Yujia Liu), Y.L. (Yang Liu) and X.D.; resources, X.L.; data curation, L.K.; review and editing, S.W.; supervision, F.M.; project administration and funding acquisition, B.H. All authors have read and agreed to the published version of the manuscript.

Funding: This project was supported by the National Science Foundation of China (51777130), Key Laboratory of Special Machine and High Voltage Apparatus (Shenyang University of Technology), Ministry of Education (KFKT202111), and Shandong Provincial Natural Science Foundation (ZR2021ME057).

Institutional Review Board Statement: Not applicable.

Informed Consent Statement: Not applicable.

Data Availability Statement: Not applicable.

Conflicts of Interest: The authors declare no conflict of interest.

References

1. Li, X.W.; Zhao, H. Review of research progress in SF_6 substitute gases. *High Volt. Eng.* **2016**, *42*, 1695–1701.
2. Zhou, W.J.; Zheng, Y.; Yang, S.A. Research progress and trend of SF_6 alternative with environment friendly insulation gas. *High Volt. Appar.* **2016**, *52*, 8–14.
3. Li, W.; Zhao, X.X.; Fu, M. Research and application progress of environmental protection insulating gas C_4F_7N Part I: Insulation and electrical and thermal decomposition characteristics. *Ransactions China Electrotech. Soc.* **2021**, *36*, 3535–3552.
4. Rabie, M.; Franck, C.M. Assessment of eco-friendly gases for electrical insulation to replace the most potent industrial greenhouse gas SF_6. *Environ. Sci. Technol.* **2018**, *52*, 280–369.
5. Zhou, Z.; Han, D.; Zhao, M.Y. Review on decomposition characteristics of SF_6 alternative gases. *Trans. China Electrotech. Soc.* **2020**, *35*, 4998–5014.
6. Meng, W.D.; Chang, Y.; Yin, F.Y. Research of C_4F_7N/CO_2, $C_5F_{10}O/C_6F_{12}O$/air environmental insulation gases performance and its application. *High Volt. Appar.* **2020**, *56*, 15–22.
7. Hu, P.; Ji, X.; Zhang, W.B. Study on lightning impulse insulation characteristics of C_4F_7N/CO_2 binary gas mixture. *High Volt. Appar.* **2021**, *57*, 1–5.
8. Song, J.J.; Zhang, Q.F.; Li, X.A. Effect of buffer gas on lightning impulse discharge characteristics and defect tolerance characteristics of C_4F_7N gas mixture. *Power Syst. Technol.* **2021**, *45*, 1626–1631.
9. Zhang, Z.; Lin, X.; Yu, W.C. Calculation of thermodynamic physical parameters of C_4F_7N/CO_2 and C_4F_7N/N_2 gas mixtures. *High Volt. Eng.* **2020**, *46*, 250–256.
10. Zhang, X.; Chen, Q.; Zhang, J. Experimental study on power frequency breakdown characteristics of C_4F_7N/CO_2 gas mixture under quasi-homogeneous electric field. *IEEE Access* **2019**, *7*, 19100–19108.
11. Ma, Y.; Liu, Y.F.; Gao, S. Detection of C_4F_7N/CO_2 Based on Fourier infrared spectroscopy. *High Volt. Appar.* **2021**, *57*, 198–204.
12. Li, W.; Zhang, X.X.; Fu, M.L. Research and application progress of environmental protection insulating gas C_4F_7N Part II: Material compatibility, safety and equipment developmen. *Ransactions China Electrotech. Soc.* **2021**, *36*, 4567–4579.
13. Li, Y.; Zhang, X.; Xiao, S. Decomposition Properties of C_4F_7N/N_2 Gas Mixture: An Environmentally Friendly Gas to Replace SF_6. *Ind. Eng. Chem. Res.* **2018**, *57*, 5173–5182. [CrossRef]
14. Tu, Y.P.; Ai, X.; Cheng, Y. DC breakdown characteristics of C_3F_7CN/N_2 gas mixtures. *Trans. China Electrotech. Soc.* **2018**, *33*, 5189–5195.
15. Chachereau, A.; Hösl, A.; Franck, C.M. Electrical insulation properties of the perfluoronitrile C_4F_7N. *J. Phys. D Appl. Phys.* **2018**, *51*, 1361–1461. [CrossRef]
16. Xiong, J.Y.; Zhang, B.Y.; Li, X.W. Study on measurements of swarm parameters in SF_6 alternative gases by pulsed townsend method. *Proc. CSEE* **2021**, *41*, 759–769.
17. Wang, L.Z.; Zhou, W.J.; Zhang, H.T. Power frequency insulation performance of C_4F_7N/CO_2 mixture under uniform and extremely uniform electric field. *High Volt. Eng.* **2019**, *45*, 1101–1107.
18. Zhang, B.; Uzelac, N.; Cao, Y. Fluoronitrile/CO_2 mixture as an ecofriendly alternative to SF_6 for medium voltage switchgears. *IEEE Trans. Dielectr. Electr. Insul.* **2018**, *25*, 1340–1350. [CrossRef]
19. Yan, X.l.; Zheng, Y.; Huang, H. Sensitivity of C_4F_7N/CO_2 gas mixture to partial inhomogeneous electric field. *Trans. China Electrotech. Soc.* **2020**, *35*, 43–51.
20. Zhang, T.R.; Zhou, W.J.; Wang, L.Z. Influences of electric field nonuniformity on breakdown characteristics of fluoronitriles/CO_2 gas mixtures under power frequency voltage. *High Volt. Eng.* **2020**, *46*, 1018–1026.
21. Zheng, Y.; Zhou, W.; Li, H. Experimental and calculation study on insulation strength of C_4F_7N/CO_2 at low temperature. *IEEE Trans. Dielectr. Electr. Insul.* **2020**, *27*, 1102–1109. [CrossRef]
22. Tang, N.; Gou, Z.; Zhang, B.Y. Effects of air-blowing on the arcing characteristics of CO_2 and CO_2/C_4-PFN, CO_2/C_5-PFK mixtures. *High Volt. Eng.* **2021**, *47*, 338–345.
23. Wu, Y.; Wang, C.; Sun, H. Properties of C_4F_7N-CO_2 thermal plasmas: Thermodynamic properties, transport coefficients and emission coefficients. *J. Phys. D Appl. Phys.* **2018**, *51*, 155206–155233. [CrossRef]
24. Seeger, M. Perspectives on research on high voltage gas circuit breakers. *Plasma Chem. Plasma Process.* **2015**, *35*, 527–541. [CrossRef]
25. Reichert, F.; Gonzalez, J.J.; Freton, P. Modelling and simulation of radiative energy transfer in high-voltage circuit breakers. *J. Phys. D Appl. Phys.* **2012**, *45*, 1–6. [CrossRef]
26. Zhan, J.F.; Fang, M.T.C.; Newland, D.B. Theoretical investigation of a 2kA DC nitrogen arc in a supersonic nozzle. *J. Phys. D Appl. Phys.* **1987**, *20*, 368–379. [CrossRef]
27. Deng, Y.K.; Peng, J.; Jiao, L. Calculation and Analysis of Insulation Performance of C_4F_7N-CO_2 Mixed Gas. *High Volt. Appar.* **2022**, *58*, 101–106.
28. Jiang, R.; He, B.; Zhang, J. Study on the insulation characteristics of environmentally friendly $CF_3I/N_2/CO_2$ mixed gas. *Emerg. Electr. Power Syst.* **2020**, *21*, 2020–2030. [CrossRef]
29. Nechmi, H.E.; Beroual, A.; Girodet, A. Effective ionization coefficients and limiting field strength of fluoronitriles-CO_2 mixtures. *IEEE Trans. Dielectr. Electr. Insul.* **2017**, *24*, 886–892. [CrossRef]
30. Huang, R.D.; Huang, H.H.; Fu, M.L. Simulation and Experimental Study on Arc Extinction Performance of New Eco-friendly Gas in 35 kV Circuit Breaker. *High Volt. Appar.* **2022**, *57*, 54–59.